Journal of Materials Chemistry C

Accepted Manuscript

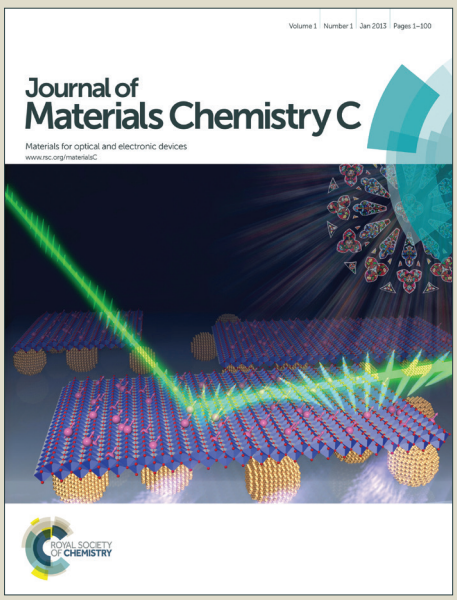

ROYAL SOCIETY OF CHEMISTRY

www.rsc.org/materialsC

Journal of Materials Chemistry C RSCPublishing

ARTICLE

The pure inorganic multi-color electrochromic thin films: vanadium-substituted Dawson type polyoxometalates based electrochromic thin films with tunable colors from transparent to blue and purple†

Cite this: DOI: 10.1039/xoxxoooooox

Received ooth January 2012,
Accepted ooth January 2012

DOI: 10.1039/xoxxoooooox

www.rsc.org/

Lin Liu,[a,b] Shi-Ming Wang, *[a] Chao Li,[a] Cheng-Gong Liu,[a] Chun-Lei Ma,[a] Zheng-Bo Han*[b]

A polyoxometalate (POM)-based pure inorganic multi-color electrochromic thin film is reported. The films are fabricated by a facile solution-based electrodeposit method. One to three vanadium atoms substituted Dawson type POMs α-$K_{6+n}[P_2W_{18-n}V_nO_{62}]\cdot 18H_2O$ (n=1, 2, 3) are used as the electrochromic materials. With the increasing of the amount of vanadium atoms in the molecule, multi-color changes are detected gradually and the performances are also enhanced with the increasing of the amount of the vanadium atoms. The tri-vanadium substituted POM-based film reveals the highest performance among the three films whose optical contrast up to 91.8 %, response time for coloration and bleaching are 3.5 s and 3.9 s, respectively. It owns coloration efficiency of 176.8 cm C^{-1} and shows maximum absorption peak shifts at 586 nm, 577 nm and 555 nm follow by the increasing of the applied potential. The performances of the films don't show obvious changes after the test of 1000 cycle's consecutive double-potential step chronoamperometric experiments which indicate the good durability.

Introduction

Electrochromic (EC) devices may be electronically darkened or lightened with small applied potentials.[1] The applications of EC devices (ECD) in anti-glare rearview mirrors, safety helmets and displays have also been reported.[2] The widespread of the ECDs depend on the synergistic cooperation of every part of the device. Electrochromic materials are the core part of the ECDs, which could be classified into three types: inorganic oxide, organic molecules and polymeric materials.[3] The inorganic oxide features high thermal stability, multi-method of processing and high performance of large optical contrast, long durability and some examples of WO_3 based electrochromic devices have already been applied in commercial area.[4] The EC based-displays could be promising alternatives to liquid crystal or light emission based displays. Tunable colors of the ECDs are another important prerequisite for their applications in displays, especially applied as the candidate of paper-like displays.[5] While compared to the organic molecules or polymeric materials, the coloration states of the inorganic EC materials are relatively monotonous. On the current state, for mono-component inorganic EC material, only single color of different extent was obtained under different applied potentials. That's to say, for mono-component inorganic EC material different colors could not be obtained by tuning the applied potentials.

There are some strategies for organic molecule or organic polymeric EC materials to obtain multicolor electrochromism, for example, grafting different functional groups to the main organic EC material through molecular tailoring; using different monomer to acquire multicolor organic polymeric EC material; and so on.[6] Though some of the organic EC materials exhibit fairish performance, the crucial issue for the organic EC materials based device is still the stability and durability.[7] And most polymeric EC materials are generally considered relatively poor photolytic stability. On the aspects of stability and durability, the traditional inorganic EC materials are more competitive to the organic EC materials.[8] However, the tuning of extrinsic colors of the mono-component inorganic EC materials seemed a challenge.[9] Therefore, the exploration of inorganic EC materials or strategies to achieve multicolor changes would be an important step to promote the application of inorganic EC materials to displays.

POMs represent a well-known class of metal oxide nanoclusters with intriguing structures and electrical properties, which have been applied in many areas such as catalysis, medicine and material science.[10] The following is a compact introduction of POMs: POMs could be deemed as the polymer of basic metal oxide cluster, such as, $\{WO_3\}$, $\{MoO_3\}$, $\{VO_3\}$, etc. Taking tungsten for example, they can form the cluster with the same kind of cluster for example $[W_{10}O_{32}]^{4-}$, which was classified as isopolyacid; if there was a different atom P or Si in

the center of some certain structures of isopolyacid, heteropolyacid was formed, such as, $[XW_{12}O_{40}]^{n-}$ (XW_{12}) or $[X_2W_{18}O_{62}]^{n-}$ (P_2W_{18}) and so on. The aforementioned structural features resulted in the devisable of the POMs. POMs could also be decorated or designed rationally to obtain certain functions.[11] More importantly, POMs were a kind of promising inorganic EC materials. Pioneered by Kurth et. al.,[12] the researches of the POMs-based EC thin layer-by-layer (LBL) films develop gradually. Like the transition metal oxide, their stability is perfect, many can retain their structure up to 500 °C. Moreover, like the organic or polymeric EC materials, the function of the POMs could be tuned through molecular design.[13] Only several groups, for example, Xu group, Ma group and Liu group have devoted in the investigation of POMs based thin EC films using LBL method.[14] POMs based multicolor EC films were also achived by the combination of POMs and another organic dye or organic EC materials by LBL method according to the color matching principle.[14h,14i] Recently, we have reported a new low cost and facile electrodeposit method to fabricate high performance POMs-based EC films. The porous TiO_2 film was used as a substrate for the loading of POMs. The EC films fabricated by electrodeposition method exhibited excellent performance that featured shorter response time, high optical contrast and high coloration efficiency.[15] Based on the devisable nature of the POMs molecules, the substituted POMs would be a proper choice to achieve the real multicolor inorganic EC materials. The substituted POMs whose metal atoms of the basic structure POMs, such as, PW_{12} or X_2W_{18} could be partly substituted by other transition metal. The transition metal substituted POMs would be helpful to break the single color change of the inorganic EC materials.

In this paper, vanadium substituted Dawson type POMs were chosen as the EC materials. To investigate the effects of vanadium atoms to the colors of EC films, three types of vanadium-substituted POMs: α-$K_{6+n}[P_2W_{18-n}V_nO_{62}]\cdot 18H_2O$ (n=1, 2, 3) were selected [abb. α-$P_2W_{18-n}V_n$ (n=1, 2, 3)]. The electrodeposit method was utlized to fabricate the film. The coloration state and the performance of the $P_2W_{18-n}V_n$ (n=1, 2, 3)-based films were also compared. With the increasing of the applied potential, only α-$P_2W_{15}V_3$-based film was observed obviously color changes from transparent, blue to purple. However, α_2-$P_2W_{17}V$ and α-$P_2W_{16}V_2$-based EC films did not show the multicolor change phenomenon obviously.

Experimental

Materials

α-$K_{6+n}[P_2W_{18-n}V_nO_{62}]\cdot 18H_2O$ (n=1, 2, 3) were prepared according to literature procedures.[16] The detail of the structure of the POMs we used was stated in the following paragraphs. The TiO_2 paste with particle size of ca. 18nm was bought from Dyesol. FTO glass (14 Ω/□, Nippon Sheet Glass) was purchased from Heptachroma (Dalian, China). The electrolyte is HCl solution (0.1 M). The other reagents were all purchased from purchased from Aladdin.

Preparation of the EC electrode

The TiO_2 film with the thickness of ca. 6 μm was prepared using the screen printing method. The electrodeposition process is as follows: the counter electrode is Pt wire; the reference electrode is SCE and the TiO_2 film acts as working electrode. The TiO_2 films are immersed in the α-$K_{6+n}[P_2W_{18-n}V_nO_{62}]\cdot 18H_2O$ (n=1, 2, 3) aqueous solution (1.0mM), the pH value of the solution was adjusted to ~2 using 1M HCl. $LiClO_4$ was employed as the supporting electrolyte and the concentration was 0.1M. Then electrodeposit using cyclic voltammogram method between -1.0 and 0.3 V at a scan rate of 100 mV s^{-1} for 30 cycles. After that, the films are rinsed with deionized water, absolute alcohol then dried with hot air. The film was placed in the oven with the temperature of 150 °C for 30min.

Film Characterization

Electrochemical experiments were performed on CHI-660D electrochemistry station (Shanghai CH Instrument Corporation, China). The films act as working electrodes; the counter electrode is Pt wire and the reference electrode is SCE. Dilute HCl (0.1M) is used as electrolyte. Scanning electron microscopy (SCE) were taken using Hitachi S-4800 scanning electron microscope. Atomic force microscopy (AFM) measurements were performed in air with a SPI3800N Probe Station. Visible light absorption spectra and transmittance spectra were obtained with a Varian Cary 500 UV-vis NIR spectrometer. IR spectra were recorded in the range of 400–2000 cm^{-1} on an Alpha Centaurt FT/IR Spectrophotometer on the Si substrate. TG analyses was performed on a Perkin–Elmer TGA7 instrument under air condition with a heating rate of 10 °C·min^{-1}.

Results and discussion

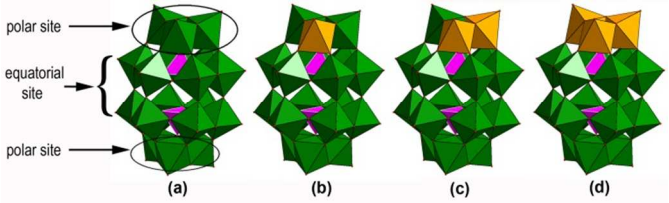

Fig. 1. The structure illustrations of the α-P_2W_{18}(a), α_2-$P_2W_{17}V$ (b), α-$P_2W_{16}V_2$ (c) and α-$P_2W_{15}V_3$ (d).

There are several isomers of the vanadium substituted Dawson type structure.[16] In order to make the different vanadium substituted POMs comparable, the substitution only occur in the same polar tungsten cluster were used in this paper. (**Fig. 1**) The structure of the vanadium substituted POMs still belongs to the saturated Dawson structure α-P_2W_{18}. For the substitution occur on the polar site, the $P_2W_{17}V$ belongs to the α_2 isomer.The stability of an EC device is in general determined by two factors: first, the stability of the EC materials; second, the stability of the EC film.[17] Specific to this paper, the stability of the vanadium substituted POMs and the interaction between POMs and the TiO_2 substrate would determine the stability of the films. The stability of the vanadium substituted POMs was tested using thermogravimetric analysis (TGA) under air condition. As shown in **Fig. S1**, the V substituted POMs are ultra-stable in the temperature scale of 50 to 600 °C, which made the V substituted POMs can be applied in large temperature scale. They also overcome the defects of low stability of the organic EC materials. The POMs-based film was fabricated using electrodeposition method as we reported before.[15] The cyclic voltammograms during preparing thin films are shown in **Fig. S2**. The peak currents density of the cyclic voltammograms increased gradually followed by the increasing of the cycles. When apporching 30 cycles, the peak current density almost become stable, which indicates that the α-$P_2W_{18-n}V_n$ (n=1, 2, 3) anions have already reached equilibration absorbed on the TiO_2. 200 cycles of consecutive CV tested was carried out to examine whether the V-POMs could form intense interactions with TiO_2 substrate. There was no sign of losing redox current intensity (shown in **Fig. S3**) observed upon performing 200 consecutive CVs. Firstly, hydrogen bonds were formed between oxygen atoms of the α-

$[P_2W_{18-n}V_nO_{62}]^{(n+6)-}$ (n=1~3) and the surface hydroxyl groups (Ti–OH) of the TiO_2 network; secondly, chemically active surface Ti–OH groups were protonated under an acidic medium to form Ti–OH_2^+ groups during the electrodeposition process. Ti–OH_2^+ group should act as a counter ion for V substituted Dawson unit and yielded the acid–base reaction. Therefore, it can be concluded that firm interaction was established between POMs molecules and TiO_2 matrix.[18] The conclusion is also confirmed by the comparison of IR spectra of the composite film, POMs and the TiO_2 substrate. As shown in **Fig. 2**, the P-O asymmetric stretching vibration of the α_2-$P_2W_{17}V$ at 1090 cm^{-1} (**Fig. 2b**) split to 3 peaks (1145, 1114 and 1086 cm^{-1} as shown in **Fig. 2c**) in the composite film. The asymmetry asymmetric stretching vibration of W-O-W, W-O-V at 1018, 954 and 920cm^{-1} also retaine in the films with some shifts. (**Fig. 2c**) The similar results were also detected in the α-$P_2W_{16}V_2$ and α-$P_2W_{15}V_3$ based composite films.[16] (as shown in **Fig. S4** and **Fig. S5**)

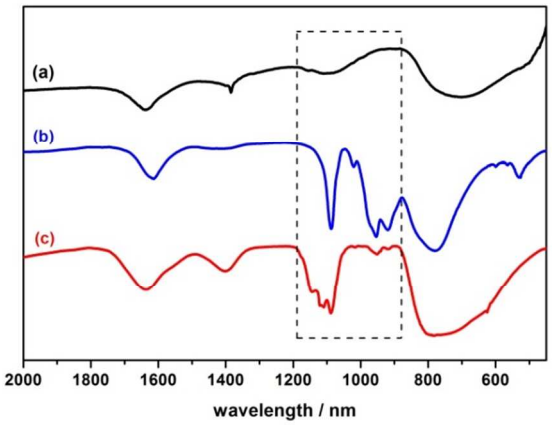

Fig. 2. The IR spectra of the TiO_2 substrate (a), the α-$K_7[P_2W_{17}VO_{62}]\cdot 18H_2O$ (b) and the composite film (c).

The surface morphology and the homogeneity of the POMs-based EC film were detected by scanning electron microscope (SEM) and atomic force microscope (AFM). As shown in **Fig. S6**. The size of TiO_2 grain of the as-prepared TiO_2 substrate was circa 15nm, and there is no aggregation of the TiO_2 particles in the substrate. After the α-$[P_2W_{18-n}V_nO_{62}]^{6-}$ (n=1~3) deposited on the TiO_2 substrate, the porous structure was still retained as shown in **Fig. 3.** There was no aggregation of POMs molecules in the pores of the TiO_2 substrate which benefited for the diffusion of electrolyte in the composite films and resulted in the short response time of coloration and bleaching.[17, 19] The AFM images as shown in **Fig. 4, S7, S8** further demonstrated that there was no aggregation of POMs molecules on the surface of TiO_2 film. The thickness of the films were ca. 6 μm after POMs deposited determined by step profiler. The transparency of the films did not change after the deposition of POMs molecules. **(Fig. S9).**

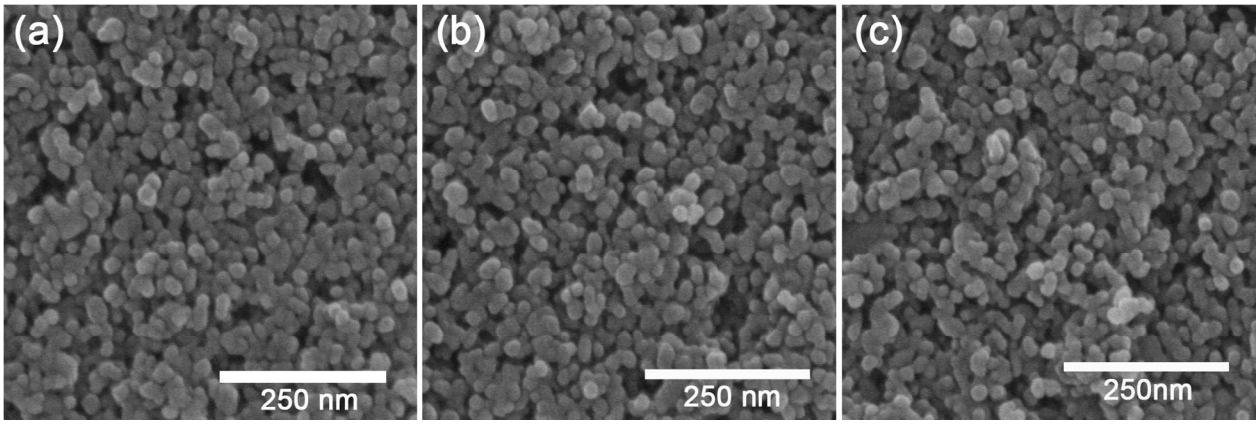

Fig. 3. The SEM pictures of the α_2-$K_7[P_2W_{17}VO_{62}]\cdot 18H_2O$-based composite film(a), the α-$K_8[P_2W_{16}V_2O_{62}]\cdot 18H_2O$-based composite film(b) and the α-$K_9[P_2W_{15}V_3O_{62}]\cdot 18H_2O$-based composite film(c).

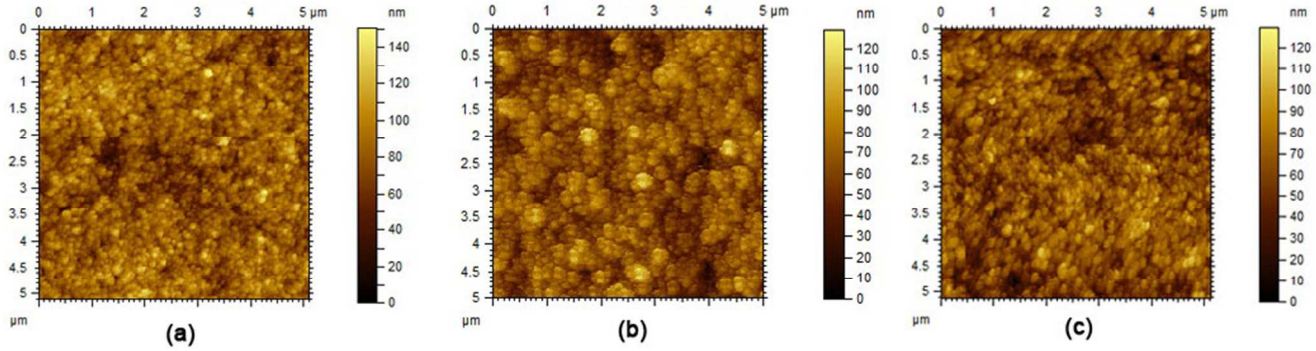

Fig. 4. The AFM results of the α_2-$K_7[P_2W_{17}VO_{62}]\cdot 18H_2O$-based composite film (a), the α-$K_8[P_2W_{16}V_2O_{62}]\cdot 18H_2O$-based composite film (b) and the α-$K_9[P_2W_{15}V_3O_{62}]\cdot 18H_2O$-based composite film (c).

The diffusion coefficient is an important parameter for the EC film, the cyclic voltammogram (CV) of the EC films under different scan rates in 0.1 M HCl aqueous solution were measured to calculate the diffusion coefficient. As shown in **Fig. 5** and **S10**, the peak current performs good linear relationship with the square root of scan rate which indicated that the reaction was fast and belonged to diffusion confined.

The diffusion coefficient (D) of H^+ ions has been calculated using Randles–Sevick's equation:[20]

$$D^{1/2} = \frac{I_p / A}{2.72\times10^5 \times n^{3/2} \times A \times C_0 \times \upsilon^{1/2}} \quad (1)$$

where I_p is the peak current density, n is the number of electrons, C_0 is the concentration of active ions in the solution, υ is the scan rate, and A is the area of the film. For an film with the area of 0.64 cm^2 and C_0 (H^+) = 0.1 M, the D value of the H^+ ions of α_2-$P_2W_{17}V$-based EC film was found to be 3.16×10^{-11} cm^2 s^{-1}; the D value of α-$P_2W_{16}V_2$-based EC electrode was 6.98×10^{-11} cm^2 s^{-1}, the D value of α-$P_2W_{15}V_3$-based EC electrode was 2.44×10^{-10} cm^2 s^{-1} The different POMs components resulted in the different D values.

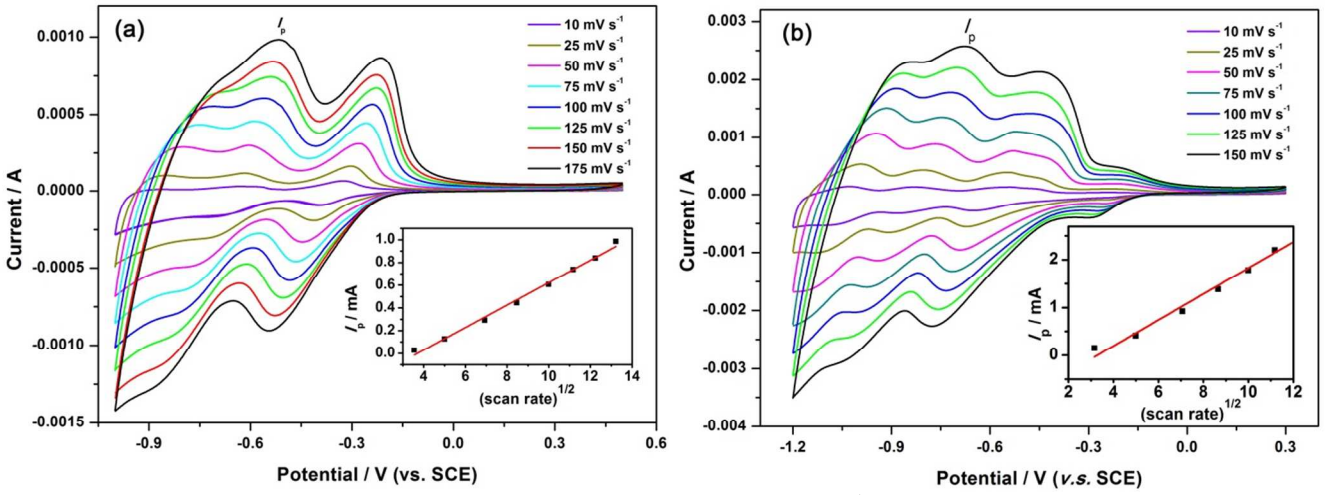

Fig. 5. Cyclic voltammograms (CVs) at different scan rates (10, 25, 50, 75, 100, 125 and 175 mV s^{-1}) of the α_2-$P_2W_{17}V$-based EC film (a) and α-$P_2W_{15}V_3$-based EC film (b) in HCl (0.1M) solution. Inset: plots of peak current versus the square root of scan rate.

It exhibited significant differences that the extrinsic hues of the coloration state of the α_2-$P_2W_{17}V$, α-$P_2W_{16}V_2$ and α-$P_2W_{15}V_3$-based EC films. The visible spectra of the $P_2W_{17}V$-based film were carried out under different applied potentials from -1.10 to -1.70 V. (**Fig. 6a**) Under the applied potential of -1.10 V the maximum ABS is 0.53 occurred at 586nm. With the increasing of the applied potential up to -1.70 V, the value of the maximum ABS has a linear increasing up to 0.844. (**Fig. 7**) The position of the maximum peaks showed a hypsochromic effect from 586 nm to 569 nm. (**Fig. 8**) Though the position of the ABS peak changes, the wavelength scale still belongs to "yellow" and the extrinsic hue of the films did not display obvious changes. For the α-$P_2W_{16}V_2$-based film, the absorption peak at the wavelength of 590 nm and did not change with the increasing of the applied potential. (**Fig. S11**) The coloration of the film exhibited a good liner relationship with the applied potential in the scale of -1.1 V to -1.6 V. However, the color would not turn deeper when the applied potential exceeded -1.6 V. The multicolor phenomenon only observed in α-$P_2W_{15}V_3$-based film. (**Fig. 6b**) Under the applied potential from -0.8 V to -1.3 V, the film showed a blue color. And the extent of the color showed good linear relationship to the applied potential. (**Fig. 7**) Within this potential region the absorption peak has a shift from 586 to 577 nm. The ABS in this region belongs to orange and the corresponding extrinsic color of the film belongs to blue. When the applied potential reached to -1.4 V, the absorption peak of the film showed a hypsochromic shift to 555 nm. With the enhancing of the potential, the position of the absorption peak restricted to 555 nm without any shift. (**Fig. 8**) The corresponding extrinsic color of the film is purple. Within the applied potential region of -1.4 to -1.8 V the extent of the color showed good linear relationship to the applied potentials. Among the three POMs based EC films, only α-$P_2W_{15}V_3$-based EC film showed obviously multicolor changes. This multi-color changes should attribute to the V substituted the W in the Dawson structure. First, the V element has EC activity. With the applied potential increasing, the W and V would be colored together which resulted in the extrinsic color of the film turn blue to purple. According to our previous research, the EC property of the saturated Daswons type POM showed relatively low performance. While, the mono-vacant lacunary Dawson structure broke the situation.[15b] According to the literature, the tri-vacant lacunary Dawson structure was unstable when dissolved in water.[21] However, the V atom occupied the lacunary sites not only stabilized the lacunary structure, but also retain the good EC properties of the lacunary Dawson structure. Second, the number of the V atoms is also important. Though the absorption peak for α_2-$P_2W_{17}V$-based film shows hypsochromic shifts, the amount of V atoms is so small that the multi-color change phenomenon could not be detected with eyes. For α-$P_2W_{16}V_2$-based film, it showed low performance and nearly no ABS peak change was detected. However, the $P_2W_{15}V_3$-based film revealed totally different results. The performance of the films was nice and the optical contrast almost exceeded the α_2-P_2W_{17}-based EC film at the applied potential of -1.7 V whose optical contrast was the highest among POMs-based EC films.[15b] What's more, the multi-color change could be detected with eyes.

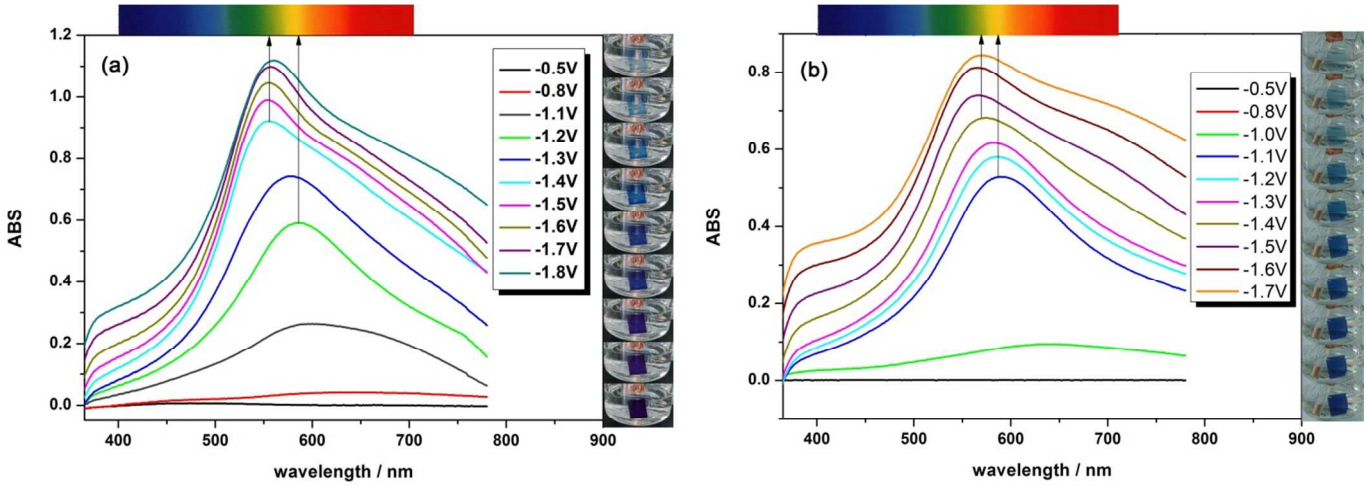

Fig. 6. (a) Visible spectra and of the α-$P_2W_{15}V_3$-based EC film under different potentials ranging from -0.5 to -1.8 V. (b) Visible spectra of the α_2-$P_2W_{17}V$-based EC film under different potentials ranging from -0.5 to -1.7 V.

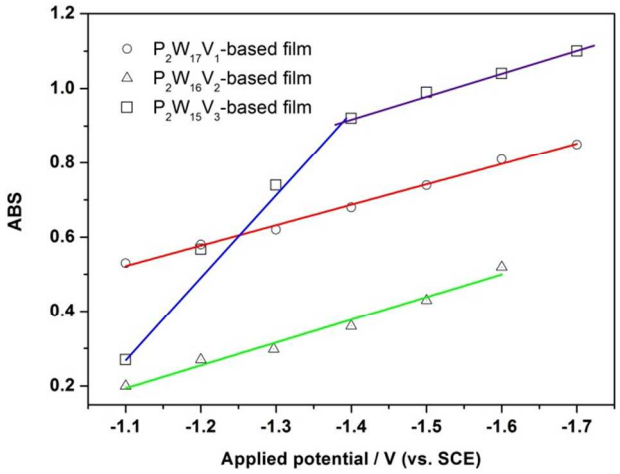

Fig. 7. The comparisons of the ABS of the three types of the EC films under different applied potentials.

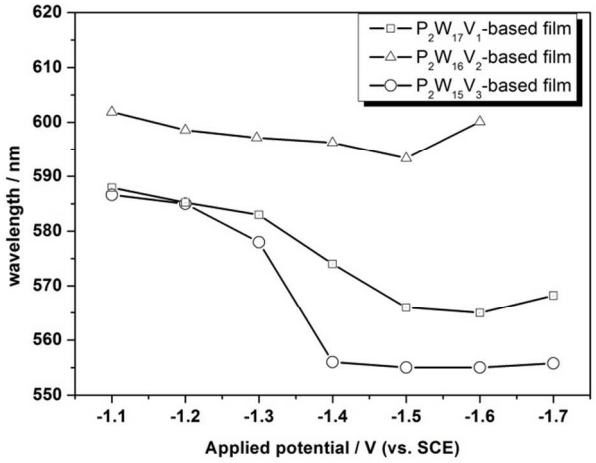

Fig. 8. The maximum ABS wavelength of the three types of the EC films.

To evaluate the performance of the devices, a double-potential step chronoamperometric experiment was done by simultaneously recording the transmittance of the device. As shown in **Fig. 9a**, the double-potential steps were -1.8~+1.3 V for α-$P_2W_{15}V_3$-based EC films. **Fig. 9b** and **9c** show the corresponding changes of the current and transmittance. The optical contrast of α-$P_2W_{15}V_3$-based EC film was 91.8 % (λ=555 nm) at the applied potential of -1.8 V. A residual leakage current rapidly achieved during coloration and the current decays rapidly to zero during bleaching for the three EC films. Similar double-potential step chronoamperometric experiments were also done to test α_2-$P_2W_{17}V$ and α-$P_2W_{16}V_2$-based EC films. The results were recorded in **Fig. S12**, the optical contrast of α_2-$P_2W_{17}V$-based EC film was 85.1% (λ=565 nm) under the double-potential steps of -1.7~+1.5 V. The optical contrast of α-$P_2W_{16}V_2$-based EC film was 48.3% (λ=590 nm) under the double-potential steps of -1.6~+1.3 V. (**Fig. S13**) The bleaching state of the films is transparent and the coloration state of the films exhibit different colors. For α_2-$P_2W_{17}V$-based film, the coloration state is deep blue; for α-$P_2W_{16}V_2$-based film, the coloration state is blue; and for α-$P_2W_{15}V_3$-based film, the coloration state is blue and purple. The stability and reversibility of the α-$P_2W_{18-n}V_n$ (n=1~3)-based EC films were also tested by repetitive double-potential step chronoamperometric. As shown in **Fig. S14**, the response time for coloration and bleaching, and the optical contrast of the α-$P_2W_{18-n}V_n$ (n=1~3)-based EC films did not change noticeably even after 10^3 cycles. It also found to be stable for more than 10^3 cycles.

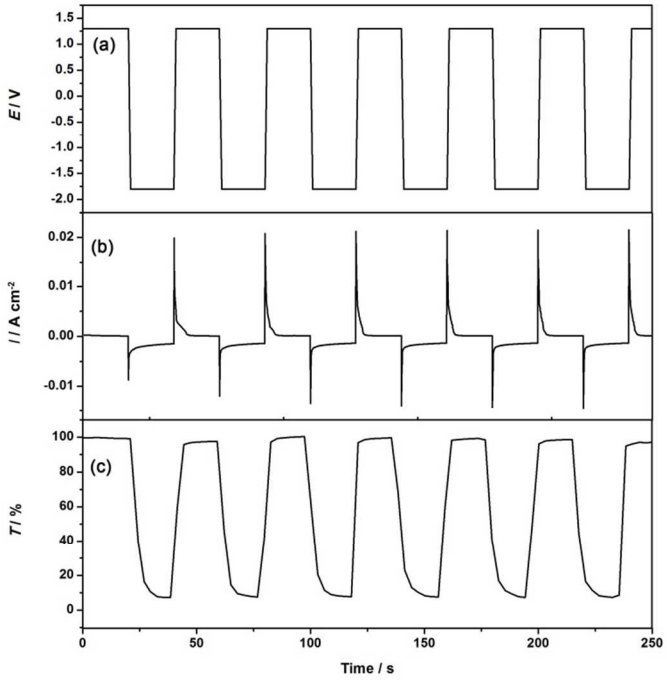

Fig. 9. Potential (a), current (b) and transmittance (c) at 620 nm of the α-$P_2W_{15}V_3$-based EC film during the subsequent double-potential step chronoamperometric of -1.8V~+1.3 V.

As shown in **Fig. 10**, the coloration/bleaching time extracted for a 90% transmittance change which was an important criterion for judging an EC film are detected to be 3.5 s ($t_{c,\ 90\%}$) and 3.9 s ($t_{b,\ 90\%}$) for the α-$P_2W_{15}V_3$-based EC film. And for the α_2-$P_2W_{17}V$-based EC film, the coloration time show a little longer than the α-$P_2W_{15}V_3$-based EC film the $t_{c,90\%}$=5.6 s, and the bleaching time $t_{b,90\%}$=4.1 s. However, the α-$P_2W_{16}V_2$-based film is more difficult to be colored and its $t_{c,\ 90\%}$ is 11.1 s and $t_{b,\ 90\%}$ is 4.5 s. The coloration efficiency (CE) is also a crucial parameter to judge an EC film which represents the change in the optical contrast (ΔOD) for the charge consumed per unit of electrode area. It can be calculated from the following formulas:[22]

$$\mathrm{CE}(\eta)=\frac{\Delta \mathrm{OD}}{q/\mathrm{S}}=\frac{\Delta \mathrm{A}}{q/\mathrm{S}}=\frac{\log(T_b/T_c)}{q/\mathrm{S}} \quad (2)$$

where ΔOD is the optical contrast at a given wavelength λ, q is injected electronic charge, S is the electrode area, ΔA is the absorbance change, T_b and T_c are the transmittances of the bleached and colored states, respectively. The CE is extracted as the slope of the line fits to the linear region of the curve. The comparison of the CE of the three types of EC films is illustrated in **Fig. 11**. The calculated CE values are 67.6, 47.8 and 176.8 $cm^2\ C^{-1}$ for α_2-$P_2W_{17}V$, α-$P_2W_{16}V_2$ and α-$P_2W_{15}V_3$-based EC films, respectively. The CE value of α-$P_2W_{15}V_3$-based EC film is the highest. The higher CE value indicated that the α-$P_2W_{15}V_3$-based EC film exhibited a large optical modulation with a small charge inserted (or extracted). In order to compare the performance of three EC films clearly, the parameters of the V-substituted POM-based EC film were also gathered in **Table 1**. It could be concluded that the V atoms in the Dawson basic structure not only affected the color modulation region of the EC films, but also affected the electrochemical properties. They all adopt the saturated structure for the three V substituted Dawson molecules. With the increase of the amount of the larger electronegative V^{5+}, it shows easier to attract electrons. But the bi-vanadium substituted α-P_2W_{18} is an exception that whose performance is the lowest. This might partly because α-$P_2W_{16}V_2$ could be regard as the combination of V_2 and the P_2W_{16} which is an unstable intermediate with low electroactivity. For α_2-$P_2W_{17}V$ and α-$P_2W_{15}V_3$, the performance was enhanced by increasing the substituted degree. The electron was first attracted by the more electronegative V^{5+} on the polar site of the Dawson anion, then the electrons pass to the W^{6+} anions on the equatorial site which are easier to be reduced than the W^{6+} anions on the polar sites. While, the α-$P_2W_{15}V_3$ has three V^{5+} to attract electrons and six vertice-shared W^{6+} anions on the equatorial site and α_2-$P_2W_{17}V$ has only one V^{5+} to attract electrons and two vertice-shared W^{6+} anions on the equatorial site. Obviously, α-$P_2W_{15}V_3$ has more EC active sites compared to α_2-$P_2W_{17}V$. Therefore, the α-$P_2W_{15}V_3$-based film is easier to be reduced, which results in shorter coloration/bleaching time of 3.5/3.9s and higher CE value of 176.8 $cm^2\ C^{-1}$.

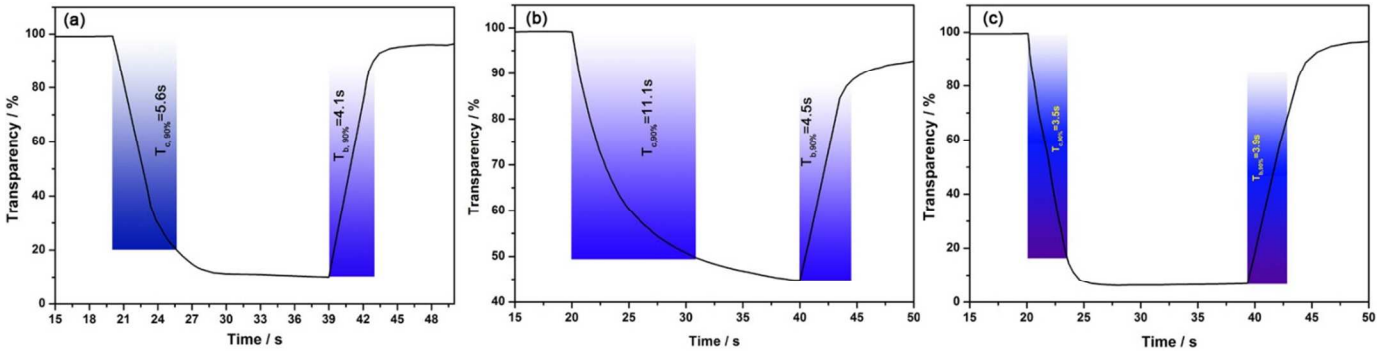

Fig. 10. The coloration/bleaching time extracted for a 90% transmittance change for the (a) α_2-$P_2W_{17}V$-, (b) α-$P_2W_{16}V_2$- and (c) α-$P_2W_{15}V_3$-based EC films.

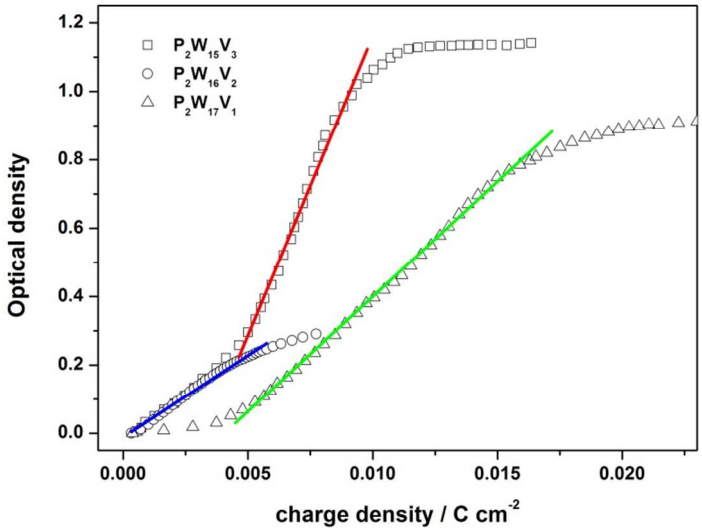

Fig. 11. The plot of optical density versus the charge density for the α_2-$P_2W_{17}V$-, α-$P_2W_{16}V_2$- and α-$P_2W_{15}V_3$-based EC films.

Table 1. Some parameters of the α_2-$P_2W_{17}V$-, α-$P_2W_{16}V_2$- and α-$P_2W_{15}V_3$-based EC films.

EC film	optical contrast$_{(max)}$	λ_{max}/ nm	color modulation	$t_{c,90\%}$ / $t_{b,90\%}$ / s	*CE* / cm^2 C^{-1}
α_2-$P_2W_{17}V$	85.1% (λ=565nm)	586, 569	transparent→ blue	5.6 / 4.1	67.7
α-$P_2W_{16}V_2$	48.3% (λ=590nm)	590	transparent→ blue	11.1 / 4.5	47.8
α-$P_2W_{15}V_3$	91.8% (λ=555nm)	586, 577, 555	transparent→ blue→ purple	3.5 / 3.9	176.8
α-P_2W_{18}*	48.7% (λ=646nm)	646	transparent→ blue	0.97 / 1.98	176.8
α_2-P_2W_{17}*	93.1% (λ=620nm)	620	transparent→ blue	0.90 / 2.81	205.3

*the data originate from **ref. 15b**

Conclusions

In conclusion, multi-color pure inorganic EC films have been prepared successfully for the first time. Color modulation from transparent to blue and purple achieved by using an electrodeposit film of α-$P_2W_{15}V_3$ as EC material and nano-TiO_2 as substrate. The structures of the V-substituted Dawson POMs (α_2-$P_2W_{17}V$, α-$P_2W_{16}V_2$ and α-$P_2W_{15}V_3$) are nearly the same but only the tri-vanadium substituted structure α-$P_2W_{15}V_3$ showed multi-color modulation. Therefore, adjusting the components of a POM molecule is an effective strategy to find new POMs-based inorganic EC materials, especially the multi-color modulation EC materials. The multi-color inorganic POMs-based EC films have great potential to be applied in EC displays. This may be an important breakthrough in inorganic EC materials area. The POMs-based films with other colors are under investigation.

Acknowledgements

This work was financially supported by National Natural Science Foundation of China (51102125), the Liaoning Province Doctor Startup Fund (20141052), the Natural Science Foundation of Liaoning (201102081) and the Youth Science Research Foundation of Liaoning University (2013LDQN19 and LDGY201412).

Notes and references

[a] Light Industry College, College of Chemistry, Liaoning University, Shenyang 110036, China; E-mail: wangsm383@163.com
[b] College of Chemistry, Liaoning University, Shenyang 110036, China.

† Electronic Supplementary Information (ESI) available. See DOI: 10.1039/b000000x/

1 a) C. M. Lampert, *Sol. Energy Mater. Sol. Cells* 2003, **76**, 489; b) M. Green, K. Pita, *Sol. Energy Mater. Sol. Cells* 1996, **43,** 393; c) D. T. Gillaspie, R.C. Tenent, A. C. Dillon, *J. Mater. Chem.*, 2010, **20**, 9585; e) K. Wang, H. Wu, Y. Meng, Y. Zhang, Z. Wei, *Energy Environ. Sci.* 2012, **5**, 8384.

2 a) H. J. Byker, J. H. Bechtel, *US. 4,917,477,* 1990; b) C. G. Granqvist, *Nat. Mater.* 2006, **5**, 89; c) T. Kobayashi, H. Yoneyama, H. Tamura, *J. Electroanal. Chem. Interfacial Electrochem.* 1984, **161**, 419.

3 a) C. G. Granqvist, *Adv. Mater.* 2003, **15**, 1789; b) J. Zhang, J. P. Tu, X. H. Xia, X. L. Wang, C. D. Gu, *J. Mater. Chem.* 2011, **21**, 5492; c) W. Lu, A. G. Fadeev, B. Qi, E. Smela, B. R. Mattes, J. Ding, G. M. Spinks, J. Mazurkiewicz, D. Zhou, G. G. Wallace, D. R. MacFarlane, S. A. Forsyth, M. Forsyth, *Science* 2002, **297**, 983. d) P. M. Beaujuge, S. Ellinger, J. R. Reynolds, *Nat. Mater.* 2008, **7**, 795.

4 E. S. Lee, D. L. DiBartolomeo, *Sol. Energy Mater. Sol. Cells* 2002, **71**, 465.

5 a) C. G. Granqvist, *Sol. Energy Mater. Sol. Cells* 2000, **60**, 201; b) U. Bach, D. Corr, D. Lupo, F. Pichot, M. Ryan, *Adv. Mater.* 2002, **14**, 845.

6 a) K. Wang, T. Zhang, Y. Hu, W. Yang, Y. Shi, *Electrochim. Acta* 2014, **130**, 46; b) G. F. Cai, J. P. Tu, D. Zhou, J. H. Zhang, X. L. Wang, C. D. Gu, *Sol. Energy Mater. Sol. Cells* 2014, **122**, 51; c) Y. W. Chuang, H. J. Yen, J. H. Wu, and G. Sh. Liou, *Appl. Mater. Interfaces* 2014, **6**, 3594; d) J. Sun, X. Lv, P. Wang, Y. Zhang, Y. Dai, Q. Wu, M. Ouyang and C. Zhang, *J. Mater. Chem. C*, 2014, **2**, 5365; e) A. A. Argun, P. H. Aubert, B. C. Thompson, I. Schwendeman, C. L. Gaupp, J. Hwang, N. J. Pinto, D. B. Tanner, A. G. MacDiarmid, and J. R. Reynolds, *Chem. Mater.* 2004, **16**, 4401. f) Y. Y. Song , Z. D. Gao , J.

H. Wang, X. H. Xia , and R. Lynch, *Adv. Funct. Mater.* 2011, **21**, 1941; g) J. Matsui, R. Kikuchi, and T. Miyashita, *J. Am. Chem. Soc.* 2014, **136**, 842.

7 J. Zhang, J. Tu, Dong Zhang, Y. Qiao, X. Xia, X. Wang and C. Gu, *J. Mater. Chem.* 2011, **21**, 17316.

8 a) D. T. Gillaspie, R. C. Tenent and A. C. Dillon, *J. Mater. Chem.*, 2010, **20**, 9585; b) P. R. Somani, S. Radhakrishnan, *Mater. Chem. Phy.* 2002, **77**, 117.

9 G. Cai, J. Tu, D. Zhou, J. Zhang, Q. Xiong, X. Zhao, X. Wang, and C. Gu, *J. Phys. Chem. C.* 2013, **117**, 15967.

10 a) H. Lv, W. Guo, K. Wu, Z. Chen, J. Bacsa, D. G. Musaev, Y. V. Geletii, S. M. Lauinger, T. Lian, and C. L. Hill, *J. Am. Chem. Soc.*, 2014, **136**, 14015; b) X. B. Han, Z. M. Zhang, T. Zhang, Y. G. Li, W. Lin, W. You, Z. M. Su, and E. B. Wang, *J. Am. Chem. Soc.* 2014, **136**, 5359; c) Q. Tang, Y. Liu, S. Liu, D. He, J. Miao, X. Wang, G. Yang, Z. Shi, and Z. Zheng, *J. Am. Chem. Soc.* 2014, **136**, 12444; d) J. Borges, L. C. Rodrigues, R. L. Reis and J. F. Mano, *Adv. Funct. Mater.* 2014, **24**, 5624; e) D. Zhou and B. H. Han, *Adv. Funct. Mater.* 2010, **20**, 2717; f) C. L. Hill, *Chem. Rev.* 1998, **98**, 1; g) T. R. Zhang, S. Q. Liu, D. G. Kurth, C. F. J. Faul, *Adv. Funct. Mater.* 2009, **19**, 642; h) A. Proust, R. Thouvenot, P. Gouzerh, *Chem. Commun.* 2008, 1837; i) S. M. Wang, L. Liu, W. L. Chen, Z. M. Su, E. B. Wang, and C. Li, *Ind. Eng. Chem. Res*. 2014, **53**, 150; j) S. M. Wang, L. Liu, W. L. Chen, E. B. Wang, Z. M. Su, *Dalton Trans.* 2013, **42**, 2961.

11 D. L. Long, E. Burkholder and L. Cronin, *Chem. Soc. Rev.* 2007, **36**, 105.

12 S. Liu, D. G. Kurth, H. Möhwald, D. Volkmer, *Adv. Mater.* 2002, **14**, 225

13 a) X. Lopez, J. J. Carbo, C. Bo, J. M. Poblet, *Chem. Soc. Rev.* 2012, **41**, 7537; b) W. G. Klemperer, in *Inorganic Syntheses*, John Wiley & Sons, Inc., Hoboken, NJ, USA 2007, Ch15; c) O. Oms, A. Dolbecq, P. Mialane, *Chem. Soc. Rev.* 2012, **41**, 7497; d) U. Kortz, A. Müller, J. Slageren, J. Schnack, N. S. Dalal, M. Dressel, *Coordin. Chem. Rev.* 2009, **253**, 2315.

14 a) S. Liu, L. Xu, F. Li, W. Guo, Y. Xing, Z. Sun, *Electrochim. Acta* 2011, **56**, 8156; b) B. Xu, L. Xu, G. Gao, Y. Jin, *Appl. Surf. Sci.* 2007, **253**, 3190; c) L. Jin, Y. Fang, P. Hu, Y. Zhai, E. Wang, S. Dong, *Chem. Commun.* 2012, **48**, 2101; c) L. H. Bi, W. H. Zhou, J. G. Jiang, S. J. Dong, *J. Electrochem. Soc.* 2008, **624**, 269; d) C. Li, K. P. O'Halloran, H. Ma, S. Shi, *J. Phys. Chem. B* 2009, **113**, 8043; e) S. Liu, Z. Tang, *Nano Today* 2010, **5**, 267; f) A. Kuhn, F. C. Anson, *Langmuir* 1996, **12**, 5481; g) I. Moriguchi, J. H. Fendler, *Chem. Mater.* 1998, **10**, 2205; h) B. Xu, L. Xu, G. Gao, Y. Yang, W. Guo, S. Liu and Z. Sun, *Electrochim. Acta* 2009*,* **54***,* 2246; i) S. Liu, L. Xu, G. Gao and B. Xu, *Thin Solid Film* 2009*,* **517***,* 4668.

15 a) S. M. Wang, L. Liu, W. L. Chen, Z. M. Zhang, Z. M. Su and E. B. Wang, *J. Mater. Chem. A*, 2013, **1**, 216. b) S. M. Wang, L. Liu, W. L. Chen, E. B. Wang, *Electrochim. Acta* 2013, **113**, 240.

16 a) S. P. Harmalker, M. A. Leparulo, and M. T. Pope, *J. Am. Chem. Soc.* 1983, **105**, 4286; b) M. Abbessi, R. Contant, R. Thouvenot, and G. Hervé, *Inorg. Chem.* 1991, **30**, 1695.

17 a) H. Zheng, J. Z. Ou, M. S. Strano, R. B. Kaner, A. Mitchell, K. Kalantar-zadeh, *Adv. Funct. Mater.* 2011, **21**, 2175; b) C. G. Granqvist, *Thin Solid Films* 2014, **564**, 1.

18 L. Li, Q.Y. Wu, Y. H. Guo, C. W. Hu, *Micropo. Mesopo. Mater.* 2005, **87**, 1.

19 a) C. S. Hsu, C. K. Lin, C. C. Chan, C. C. Chang, C. Y. Tsay, *Thin Solid Films* 2006, **494**, 228; b) H. Huang, J. Tian, W. K. Zhang, Y. P. Gan, X. Y. Tao, X. H. Xia, J. P. Tu, *Electrochim. Acta* 2011, **56**, 4281; c) B. Baloukas, J. M. Lamarre, L. Martinu, *Sol. Energy Mater. Sol. Cells* 2011, **95**, 807.

20 a) S. S. Kalagi, S. S. Mali, D. S. Dalavi, A. I. Inamdar, H. Im, P. S. Patil, *Synthetic Met.* 2011, **161**, 1105; b) S. S. Kalagi, S. S. Mali, D. S. Dalavi, A. I. Inamdar, H. Im, P. S. Patil, *Electrochim. Acta* 2012, **85**, 501.

21 R. Contant, W. G. Klemperer, and O. Yaghi, in *Inorganic Syntheses*, John Wiley & Sons, Inc., Hoboken, NJ, USA 2007, Ch18.

22 Z. Xie, L. Gao, B. Liang, X. Wang, G. Chen, Z. Liu, J. Chao, D. Chen, G. Shen, *J. Mater. Chem.* 2012, **22**, 19904.

Table of Content

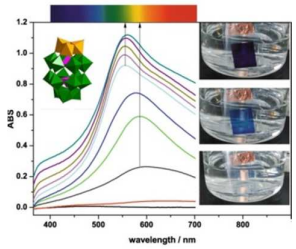

The vanadium-substituted polyoxometalates based inorganic electrochromic thin films reveal multi-color changes from transparent to blue and purple.